International Journal of Medical Toxicology & Forensic Medicine
2026, Volume 16, E53703

Research Paper

A Hybrid Transfer Learning and Broad Learning Framework for Cervical Cell Classification Using SIPaKMeD Images

Suraj Soren[1], Paidi Annan Naidu[2], Sridharan Matchidurai[3], Nune Naresh Chary[4], Varadharajan Bhoopathy[5]

1. *Department of Computer Science and Engineering, GMRIT Deemed to be University, Rajam, India.*
2. *Department of Information Technology, GMR Institute of Technology (GMRIT)-Deemed to be University, Rajam, India.*
3. *Department of Mathematics, NPR College of Engineering and Technology (Autonomous), Natham, India.*
4. *Department of Electronics and Communication Engineering, CVR College of Engineering, Hyderabad, Telangana, India.*
5. *Department of CSE, Sree Rama Engineering College, Tirupati, Andhra Pradesh, India.*

Citation Soren S, Naidu PA, Sridharan M, Chary NN, Bhoopathy V. A Hybrid Transfer Learning and Broad Learning Framework for Cervical Cell Classification Using SIPaKMeD Images. International Journal of Medical Toxicology and Forensic Medicine. 2026; 16:E53703.

https://doi.org/10.22037/ijmtfm.v16.53703

Article info:

Received: 07 October, 2026

Accepted: 22 October, 2026

Published: 01 November, 2026

Keywords:

Cervical Cell Classification, SIPaKMeD, Broad Learning System, Transfer Learning, Faster R-CNN, InceptionV2, Medical Image Analysis, Cervical Cytology

ABSTRACT

Background: Automated cervical cell image classification can support cytological screening by helping identify different cervical cell types. This study proposes a hybrid Transfer Learning and Broad Learning System (TL-BLS) framework for classifying five cervical cell classes.

Methods: We used the SIPaKMeD image collection, comprising 4,049 cervical cell images. Image preprocessing included CLAHE, bilateral filtering, Laplacian sharpening, and unsharp masking. We used Faster R-CNN with an InceptionV2 backbone for transfer-learning-based feature representation, followed by a Broad Learning System for classification. We partitioned the images into training, validation, and testing subsets using a 70%/15%/15% split. This study's main contribution is a combined framework that combines Faster R-CNN with an InceptionV2 backbone for candidate cell-region detection and feature representation, followed by a Broad Learning System (BLS) for five-class cervical cell classification. The proposed architecture integrates transfer-learning-based feature extraction with a broad-learning classifier. We report precision, recall, and F1-score using macro-averaging, the unweighted mean of the corresponding class-wise metrics.

Results: The proposed Hybrid TL-BLS framework correctly classified 578 of 609 test images, achieving 94.91% accuracy and precision, and 94.89% and 94.90% recall and F1-score, respectively.

Conclusion: The proposed framework manifests promising performance for five-class cervical cell-image classification. However, the evaluation is limited to the SIPaKMeD dataset and does not establish patient-level cervical cancer diagnosis or risk prediction. Further validation using independent and clinically representative datasets is required.

*** Corresponding Author:**
Varadharajan Bhoopathy, PhD
Department of CSE, Sree Rama Engineering College, Tirupati, Andhra Pradesh, India.
E-mail: *v.bhoopathy@gmail.com*

Copyright © 2026 The Author(s);
This is an open-access article distributed under the terms of the Creative Commons Attribution-NonCommercial 4.0 International License (CC BY-NC 4.0: https://creativecommons.org/licenses/by-nc/4.0/), which permits unrestricted non-commercial use, distribution, and reproduction in any medium, provided the original work is properly cited.

Introduction

Cervical cancer ranks as the fifth most frequently identified cancer among women worldwide [1]. The disease is closely related to HPV infection, especially HPV-16 and HPV-18 [2]. Early detection and accurate identification are important for increasing patient outcomes and reducing disease progression [3]. Cervical cancer can also cause serious complications as the disease progresses, highlighting the importance of effective screening and early diagnosis [4].

Pap smear screening is one of the commonly used methods for detecting precancerous or premalignant cervical cells through microscopic examination [5]. Liquid-based cytology (LBC) is also used as an alternative to conventional cytology because it can provide cleaner and more uniform slides for microscopic analysis [1]. However, the classification of cervical cells remains challenging because different cell types may exhibit similar morphological characteristics [6]. In particular, variations in nuclear size, cellular structure, staining characteristics, and cell appearance can make microscopic interpretation difficult. The classification process also depends on trained professionals' knowledge and experience, which may contribute to diagnostic variability. Therefore, automated approaches are required to support efficient and consistent cervical cell categorization [7].

Recent improvements in ML and DL have provided new opportunities for automated cervical image analysis. Various ML classifiers, CNN, EL approaches, and transfer learning techniques have been investigated for cervical cell classification and cervical cancer-related image analysis[4]. These approaches have demonstrated the potential of automated feature learning and classification; however, challenges remain in handling variations in cell morphology, obtaining robust feature representations, and achieving reliable generalization across different image characteristics [8].

Although previous studies have demonstrated the effectiveness of ML, CNN, EL, and transfer learning for cervical image analysis, existing approaches generally focus either on deep feature learning or conventional classification[9]. Integrating transfer-learning-based feature representation with a Broad Learning System (BLS) for five-class cervical cell classification has received comparatively little attention. This motivates the proposed Hybrid TL-BLS framework.

Existing cervical cell-classification approaches primarily rely on end-to-end deep learning architectures or conventional classifiers, and their performance can be affected by morphological similarities between cell categories. This study considers a hybrid approach that combines Faster R-CNN with an InceptionV2 backbone for region-level feature representation and BLS for final classification. The objective is to evaluate this combination for five-class cervical cell-image classification using the SIPaKMeD dataset. The contribution rests in integrating and experimentally evaluating these components, rather than claiming that either component is independently novel.

In this paper, the automated classification of cervical cell images is performed using SIPaKMeD dataset[10]. The proposed framework uses image preprocessing, feature extraction, transfer learning using Faster R-CNN with an InceptionV2 backbone, and BLS-based classification. The study considers five cervical cell categories, which include Dyskeratotic, Koilocytotic, Metaplastic, Parabasal, and Superficial-Intermediate. The proposed framework is evaluated using some evaluation metrics, and the confusion matrix analysis is compared with selected classification approaches.

Cervical cancer image analysis has been investigated using a variety of Machine Learning and DL techniques [11]. Early machine learning approaches primarily relied on manually extracted image and clinical features followed by conventional classifiers. SVM has been widely investigated for cervical image and medical-image classification, particularly in situations involving limited training samples [7–11]. Its ability to construct effective decision boundaries for nonlinear classification problems has made it a commonly investigated approach for medical image analysis.

Ensemble learning approaches have also been explored to improve classification performance by concatenating multiple learning models and feature-selection strategies [5]. Such approaches can exploit complementary characteristics of different models. However, their performance depends on the quality of the extracted features and the classifiers used.

Other machine learning approaches have explored ANN, KNN, fuzzy-based methods, and multilayer perceptron (MLP) models for cervical cell and cervical cancer classification [17–21]. These studies demonstrate the applicability of machine learning for identifying cervical abnormalities using morphological, color, texture, and other image-derived

characteristics. However, conventional approaches often rely on handcrafted feature representations and have limited capacity to capture complex cellular patterns directly from images.

With the development of DL, CNNs and TL approaches have increasingly been applied to cervical image analysis [12]. Deep learning models can automatically extract hierarchical feature representations from input images and reduce dependence on manually designed features. Transfer learning is particularly useful when the target medical-image dataset is relatively limited because pretrained representations can be adapted to the target task [13]. Nevertheless, the performance of deep architectures can be influenced by dataset characteristics, class similarity, and the generalization of learned representations.

Broad Learning System (BLS) provides an alternative learning strategy in which feature representations are expanded through mapped feature nodes and enhancement nodes rather than relying entirely on increasing network depth. BLS has been applied to classification problems and provides an efficient broad feature representation [14]. However, the integration of transfer-learning-based feature representation with BLS for five-class cervical cell classification has received comparatively limited attention.

Previous studies have explored conventional machine learning, CNN-based classification, transfer learning, and ensemble architectures for cervical cell-image analysis. However, their reported performance cannot be compared directly without considering dataset composition, data partitioning, preprocessing, and evaluation protocols [4]. The present study evaluates a combination of Faster R-CNN with InceptionV2 and BLS for five-class classification. A comparative summary should identify each study's dataset, method, reported metrics, and principal limitations using verified information from the cited publications.

Existing approaches generally focus either on deep feature learning or conventional classification, whereas the integration of transfer-learning-based region representation with a Broad Learning System for five-class cervical cell classification has received comparatively limited attention. This motivates the proposed Hybrid TL-BLS framework.

Our two-stage framework for cervical cell-region representation and five-class classification is outlined in this article. In terms of cervical cancer early detection, this can be seen as beneficial support. Key contributions include the following.

- For the effective management of cervical cancer, this article suggests a two-step process. The Faster RCNN framework is investigated, using InceptionV2 for predetection and BLS for verification. Two steps work together to prove its efficacy.

- Through a thorough examination, we demonstrate enhanced diagnostic accuracy and robustness by validating our technique with the SIPaKMeD dataset. The procedure produced 966 images of cluster cells and 4,049 images of single cells. Isolated cell images with dimensions varying from 71×59 pixels to a maximum width of 531×278 pixels and $height\ of\ 388 \times 553$ pixels were included in the input.

- The proposed framework is compared using quantitative classification analysis and is compared with selected existing classification architectures.

Materials and Methods

The proposed Hybrid Transfer Learning and Broad Learning System (TL-BLS) framework is designed for five-class cervical cell-image classification using the SIPaKMeD dataset. The overall framework consists of four major stages: (1) image preprocessing, (2) transfer-learning-based feature representation and candidate cell-region detection using Faster R-CNN with an InceptionV2 backbone, (3) Broad Learning System (BLS)-based feature representation and classification, and (4) performance evaluation using the test set.

Figure 1 depicts a schematic of our proposed system. They build an investigative framework on top of the SIPaKMeD dataset, a complete collection of cervical screening photos, in order to increase the efficiency of five-class cervical cell classification [15]. The dataset is then split into training and evaluation sets, with 70% for learning, 15% for testing, and 15% for validation.

Dataset Description

At this dataset SIPaKMeD you may get the dataset that was utilised for this study. The five distinct cell types found within are described in depth. The present study formulates the classification task as a five-class cervical cell classification problem. The five categories considered are Dyskeratotic, Koilocytotic, Metaplastic, Parabasal, and Superficial-Intermediate [10]. Cell types that are considered normal include parabasal cells and superficial intermediate cells, whereas cell types that are considered abnormal include koilocytotic,

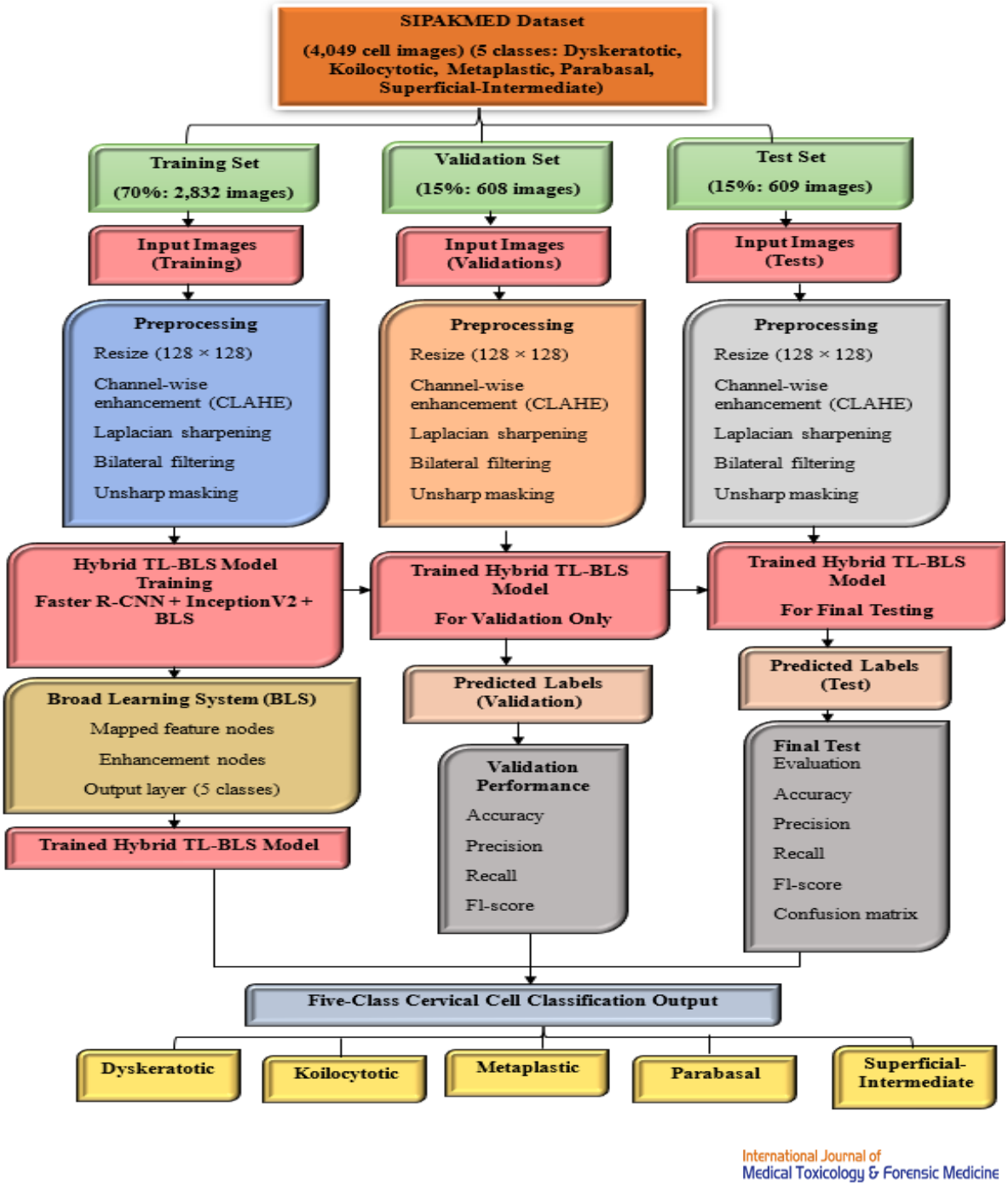


Figure 1. Overall workflow of the proposed Hybrid TL-BLS framework.

dyskeratotic, and metaplastic cells. We have established two subgroups within the normal category: parabasal cells and superficial intermediate cells. Tables 1 and 2 outline the dataset's primary features [16].

The SIPaKMeD dataset contains 966 original images and 4,049 manually classified cell images across five categories. In this study, we partitioned the cell-image dataset into training, validation, and test subsets at a 70:15:15 ratio, comprising 2,832, 608, and 609 images, respectively. Table 3 presents the class-wise distribution. The splitting procedure should explicitly state whether partitioning occurred at the original-image or cell-image level and document how related cells were kept separate to prevent data leakage.

Figure 2 displays photos from these two categories. Cervical cancer screening approaches, including Pap smear, HPV testing, and colposcopy, are extensively covered in the literature, emphasizing early diagnosis. Unfortunately, automated screening technologies using

Table 1. The Data Distribution from the SIPaKMeD.

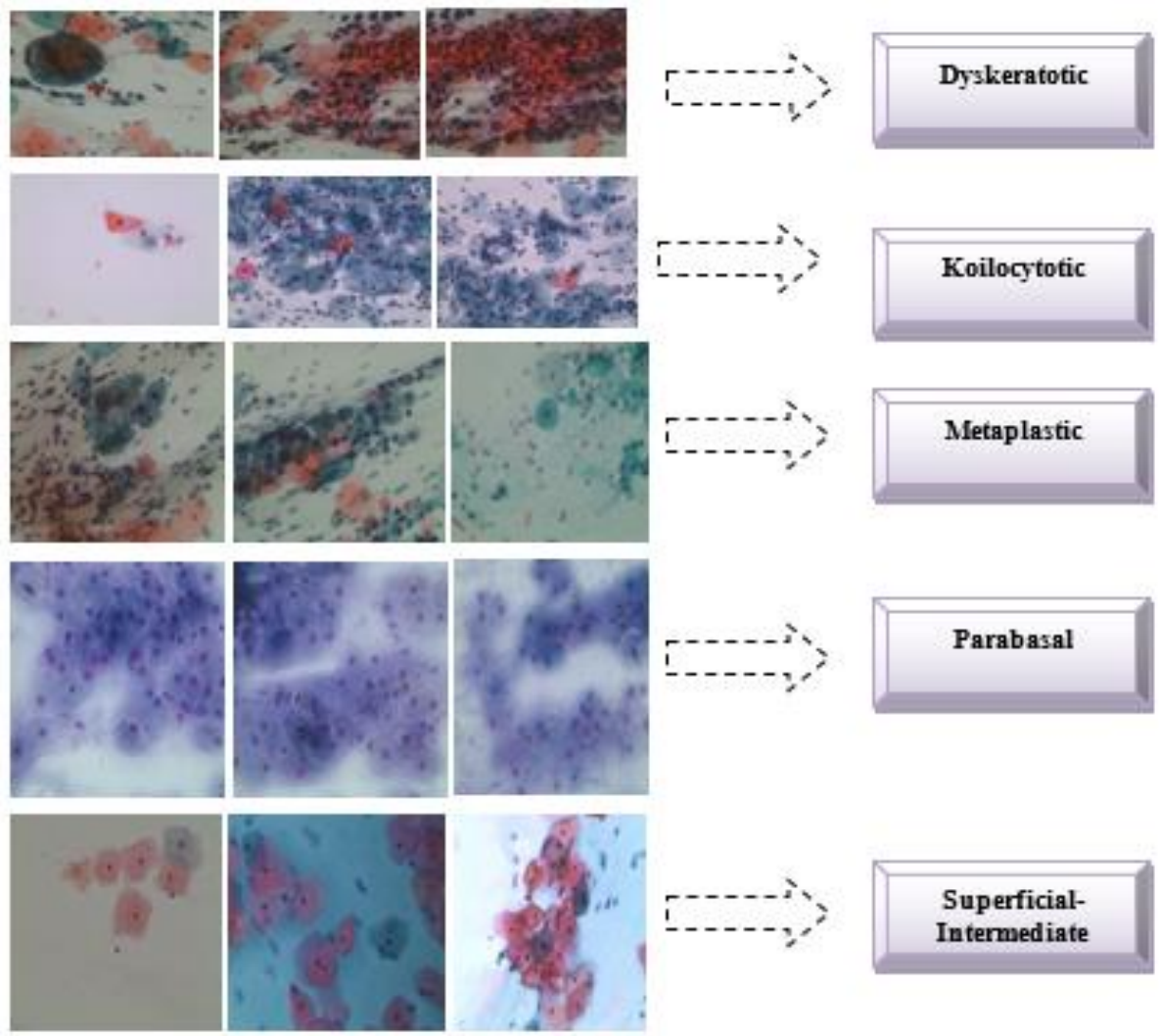
Dataset	Class	No of Images	No. of Cells
SIPaKMeD	Dyskeratotic	223	813
	Koilocytotic	238	825
	Metaplastic	271	793
	Parabasal	108	787
	Superficial-Intermediate	126	831
Total		966	4,049

Table 2. Detail Properties SIPaKMeD Databases. https://www.cs.uoi.gr/~marina/sipakmed.html

Property	SIPaKMeD
Data Type	Image
Cells Per Image	Variable
Image Size	2,048 × 1,536 (pixel)
Format	.bmp
No. of Images	966
Data Acquisition	Pap-Smear
Classification	Manual
Class	5
Classified Cells	4,049
Validation	Expert Cytopathologists

International Journal of
Medical Toxicology & Forensic Medicine

International Journal of
Medical Toxicology & Forensic Medicine



International Journal of
Medical Toxicology & Forensic Medicine

Figure 2. SIPaKMeD Dataset Sample Images.

Pap smear pictures are lacking.

Preprocessing

As seen, the pre-processing procedure consists of multiple steps. What follows is a description of the steps:

Resizing and Splitting

In order to accommodate some DL models, the

images were downsized to 128 x 128. The memory overflow in our fusion-based model when it used the standard 224×224 input led us to choose this size as an optimal compromise between computational performance and memory limitations. We then divided the resized images into green, red, and blue channels [17]. The Hybrid TL and BLS model performed poorly and produced poor visual quality in experiments that included preprocessing procedures such as CLAHE, Laplacian sharpening, bilateral filter, and unsharp masking on the whole images. To improve performance, they investigated channel-wise preprocessing by testing different combinations, such as red-green-blue. The highest-quality results and most noticeable performance boosts came from preprocessing each of the three channels independently.

CLAHE

By implementing Contrast Limited Adaptive Histogram Equalization (CLAHE), the noise level in the images was reduced while the contrast was enhanced. It was initially used to fix uneven lighting throughout the image and to enhance local contrast in poorly illuminated regions before subsequent processing could eliminate it. Experiments were conducted with clip-limit values from 1.0 to 5.0 at intervals of 0.5. The selected configuration used a clip limit of 5.0 for the red channel and 4.5 for both the green and blue channels. The selected preprocessing parameters were fixed for the subsequent experiments and applied consistently to the training, validation, and test images.

Laplacian Sharpening

Laplacian kernels were applied to the CLAHE output for detecting edges and for brightening the images. The size of the kernel was set to 3. A 3 × 3 kernel was used for this operation, which is the Laplacian kernel [[-1, -1, -1], [-1, 9, -1], [-1, -1, -1]]. Laplacian sharpening, when applied after CLAHE, helps to restore images that have been softened or blurred by bringing back details and edges that may have been lost during local contrast enhancement.

Bilateral Filter

To counteract the over-sharpening of undesirable areas, we utilized bilateral filtering to make the photos smoother while keeping their edges. The image that has been Laplacian-sharpened is first subjected to bilateral filtering. The difference between the denoised image and the original image is calculated. The image that has been enhanced using CLAHE now includes this distinction. By enhancing contrast with the CLAHE output and restoring clarity through denoising, this technique improves image detail. By combining Laplacian sharpening with bilateral filter denoising, this method recovered regions that had previously been rejected. After that, a single RGB image was created by combining the output channels.

Unsharp Masking

We produced an unsharp-masked output image by applying a Gaussian blur to the original image and then subtracting the blurred version from the merged output image. α=3, β=-3, γ=50, and σ= 30 are the unsharp masking values that were utilized. To highlight broader image structures and reduce fine noise, the resized input is subjected to a Gaussian blur with σ=30. Overall, this removes any remaining noise and highlights the image's fine features.

Hybrid TL and BLS

The proposed combined framework consists of two sequential stages. First, the Faster R-CNN model with an InceptionV2 backbone performs region proposal and detection to identify candidate cellular regions. Second, the extracted candidate representations are passed to the Broad Learning System for verification and final classification. Thus, the Faster R-CNN stage performs region-level feature learning and localization, whereas the BLS stage performs the final classification of the detected cell category.

The proposed framework operates in two sequential stages. First, Faster R-CNN uses the InceptionV2 backbone to extract hierarchical feature maps and generate candidate cell regions through its region proposal network. Region-level representations are obtained from the selected proposals and converted into feature vectors suitable for classification. These feature vectors are then supplied to the BLS, which constructs mapped feature nodes and enhancement nodes before producing the final five-class prediction. The detector and classifier therefore perform complementary region-representation and classification functions.

Redetection for Hybrid TL Model

For five-class cervical cell screening, they create a deep TL model. The area of focus is five-class cervical cells. It requires a model that can accurately suggest effective regions to detect those ROIs. The Faster R-CNN framework's region proposal network (RPN) can generate a number of potential regions for further evaluation. The framework subsequently generates candidate regions along with their corresponding classification scores. For this reason, it serves our

purpose well as a predetection module. Finding as many returns on investment (ROIs) as feasible is the main principle of this stage. The predetection process consists of the following four stages:

Extract Feature Maps

The feature maps are extracted via a sequence of convolutional operations, followed by pooling and relu layers. Following the feature map's last layer, the RPN and ROI pooling processes will make use of it.

Proposal Generation

RPNs employ a feature known as an anchor generator to generate enough proposals for selection. In the proposed implementation, we use four anchor scales (0.25, 0.5, 1.0, and 2.0) and three aspect ratios (0.5, 1.0, and 2.0). The box-classification and box-regression layers are part of the RPN. The box-regression layer handles proposal placement, while the box-classification layer classifies boxes as objects or backgrounds.

Fixed Dimension of Feature Representation

ROI-pooling takes a feature map from the convolution layers and the RPN-generated suggestions, then uses max-pooling to create a fixed-dimensional feature representation for each ROI. For future regression and classification, it eliminates the need for fixed feature map sizes. The input sizes never determine the fixed feature map dimension; instead, the layer parameters do.

Object Classification and Localization

Here, they take a fixed-dimensional feature map and uses it to calculate the class probabilities. At the same time, precise box positions are obtained by the bounding box regression. The last step is to generate the predicted objects and their positions.

It is worth mentioning that RPN is a great method for providing enough suggestions. This configuration helps maintain an appropriate trade-off between computational complexity and detection performance [18]. A large number of candidate regions are produced following a simple four-step process.

InceptionV2 is employed as the backbone network of the Faster R-CNN detector to obtain hierarchical feature representations from the preprocessed cervical cell images.

Faster R-CNN with InceptionV2

For the proposed framework Faster R-CNN with an InceptionV2 backbone is used as TL componenet. The backbone extracts hierarchical feature representations from the preprocessed cervical cell images, while RPN identifies candidate regions for further analysis. RPN configuration uses four anchor scales (0.25, 0.5, 1.0, and 2.0) together with three aspect ratios (0.5, 1.0, and 2.0).

In the proposed architecture, InceptionV2 serves as the backbone for extracting hierarchical image features, while the region proposal network generates candidate regions using four anchor scales (0.25, 0.5, 1.0, and 2.0) and three aspect ratios (0.5, 1.0, and 2.0). We process the selected regions to obtain fixed-dimensional representations for subsequent classification. These representations form the input to the BLS classifier, which generates the final cell-category predictions. The implementation description should additionally specify the pretrained checkpoint, detector configuration, ROI dimensions, and feature-extraction layer used.

The RPN-generated candidate regions are processed through the ROI feature-extraction stage to obtain fixed-dimensional representations. These representations are subsequently provided to the BLS classifier for final five-class classification.

Verification of BLS

At this point, they check whether the detection results are indeed objects or just background. This is where BLS is used. The defining feature of BLS is its construction as a flat neural network. In order to classify photos, the input images are initially transformed into "mapped features," which are random feature nodes. Then, all of the mapped features are extended into "enhanced features," which are also feature nodes. To summarise, our predetection model makes use of the three modules shown in Figure 3.

Mapping-feature equation

The input feature matrix $X$is transformed into multiple groups of mapped features. The i-th group of mapped features is generated as defined in Equation (6).

$$N_j = \tau\left(WX_{nj} + \alpha_{nj}\right), j = 1,2, \dots, o \quad (6)$$

where τ is a mapping function and X_{nj} and α_{nj} are weights that are produced randomly from a given distribution.

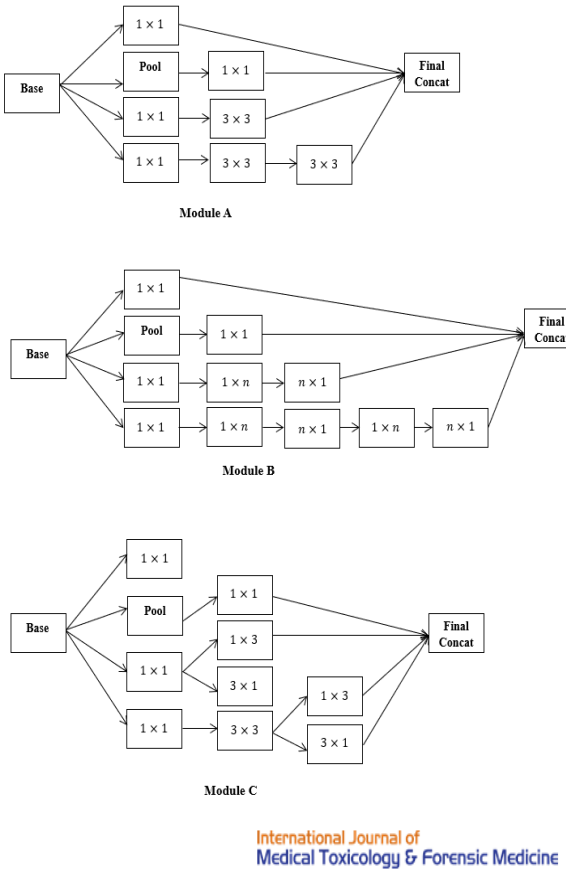


Figure 3. Three modules of the InceptionV2 structure.

Enhanced Feature Generation

A sparse autoencoder is employed to refine the mapped feature representations so that more important features can be explored. A concatenation of $N^o \equiv [N_1, \ldots, N_o]$ expresses the p groups of mapped features that are formed after a sequence of mapping operations. Equation (7) then displays the extended features that have been processed.

$$F_i = \pi\left(N^o X_{fi} + \alpha_{fi}\right), i = 1,2, \ldots, R \qquad (7)$$

For example, where π is an activation function that is not linear. The words X_{fi} and α_{fi} mean weights that are produced from a specific distribution. $F^r \equiv [F_1, \ldots F_r]$ expresses the first r groups of enhanced nodes.

BLS combined representation

The output layer is simultaneously related to all the mapped features, and improved features are shown in Equation (8).

$$Z = [N_1, N_2, \ldots, N_o, F_1, F_2, \ldots, F_r]\, X = [N^o | F^r] X \qquad (8)$$

where Z stands for output and X represents the weights of the entire network.

Results

For reproducibility, the SIPaKMeD dataset was divided into training, validation, and test subsets using a 70%/15%/15% split, respectively. The random state option was set to 42. In Table 3 you can see the final datasets. Various preprocessing methods were applied after the data was divided. Meanwhile, we made sure that all images had the original aspect ratio and the same dimensions by immediately preprocessing the data using CLAHE, Resizing and Splitting, Laplacian Sharpening, unsharp masking, and bilateral filtering.

Table 3. Summary of the Dataset.

Class	Training	Validation	Testing
Dyskeratotic	569	122	122
Koilocytotic	577	124	124
Metaplastic	555	119	119
Parabasal	550	118	119
Superficial-Intermediate	581	125	125
Total	2,832	608	609

International Journal of Medical Toxicology & Forensic Medicine

Figure 4 shows the classification results obtained by the proposed Hybrid TL-BLS framework on the test set. The proposed Hybrid TL-BLS framework correctly classified 578 of the 609 test images, yielding an accuracy of 94.91%. The confusion matrix indicates that the largest number of misclassifications occurred in the Metaplastic class, with 10 images assigned to other categories, followed by Koilocytotic, with 8 misclassified images. These errors may reflect overlapping morphological characteristics between cell categories. Precision, recall, and F1-score should be reported using the explicitly stated averaging strategy

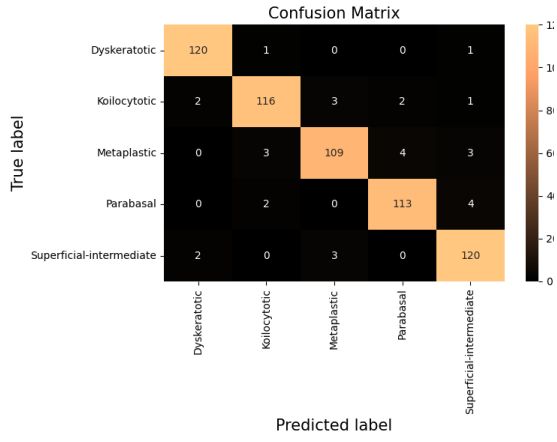


Figure 4. Confusion Matrix.

and verified against the class-wise confusion-matrix results.

Table 4 presents the reported performance of the proposed Hybrid TL-BLS framework and the selected comparison models. The proposed framework achieved the highest reported accuracy, 94.91%, among the listed methods. For a fair comparison, all models must use the same leakage-controlled dataset partition, consistent preprocessing, and identical evaluation

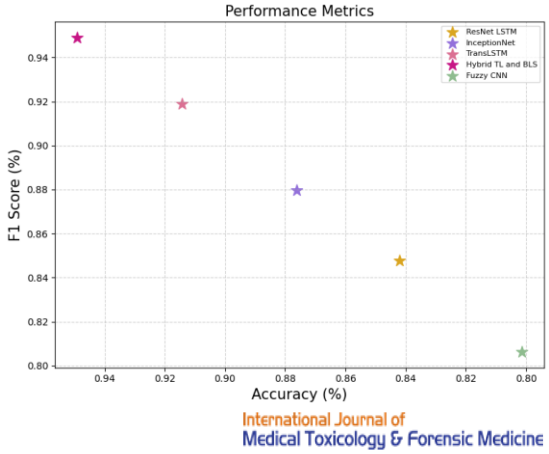
Table 4. Performance Metric.

Model	Accuracy	Precision	Recall	F1-Score
ResNet LSTM	84.21	82.11	80.34	84.76
InceptionNet	87.63	85.50	83.62	87.98
TransLSTM	91.42	89.54	87.76	91.90
Hybrid TL and BLS	94.91	94.92	94.89	94.90
Fuzzy CNN	80.14	78.84	76.62	80.61

International Journal of
Medical Toxicology & Forensic Medicine

metrics. Document the references, implementation details, and experimental conditions for each baseline to support reproducibility.

Figure 5 compares the reported F1-score and Accuracy values of the evaluated models. The Hybrid TL-BLS framework shows the highest reported accuracy among the compared methods. This evaluation is limited to the SIPaKMeD dataset and five-



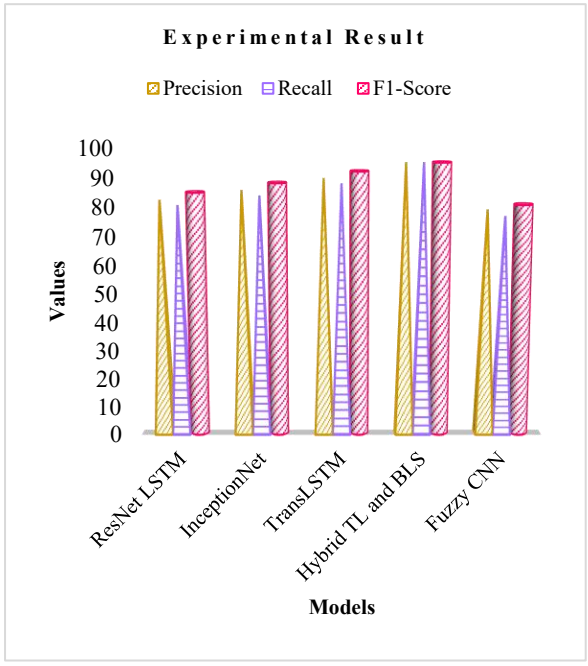
International Journal of
Medical Toxicology & Forensic Medicine

Figure 5. Accuracy versus F1-score comparison of the evaluated models.

class cervical cell image classification; therefore, the reported performance should not be interpreted as direct clinical diagnostic accuracy.

Figure 6 compares the results of a Hybrid TL-BLS for five-class cervical cell prediction. Fuzzy CNN, Hybrid TL and BLS, InceptionNet, ResNet LSTM, and TransLSTM are some of the evaluated models that have been computed using a five-class cervical cell dataset.

Figure 6 shows the Hybrid TL and BLS approach with the following metrics: F1-score of 94.9, recall of 94.89, and precision of 94.92. Alternatively, the TransLSTM



International Journal of
Medical Toxicology & Forensic Medicine

Figure 6. Experimental Result Comparison.

method's acquired metrics are displayed here: an F1-score of 91.90%, recall of 87.70%, and precision of 89.50%.

Discussion

The present study investigated a hybrid Transfer Learning and Broad Learning System (TL-BLS) framework for automated five-class cervical cell-image classification using the SIPaKMeD dataset. The proposed framework merges Faster R-CNN with an InceptionV2 backbone for candidate cell-region detection and feature representation, followed by a Broad Learning System (BLS) for final classification. The experimental findings demonstrate the potential of combining deep transfer-learning-based feature extraction with a broad-learning classification strategy for distinguishing different cervical cell categories.

The proposed Hybrid TL-BLS framework achieved an overall classification accuracy of 94.91%, correctly classifying 578 out of 609 test images. The reported precision, recall, and F1-score were approximately 94.92%, 94.89%, and 94.90%, respectively, as presented in Table 4. These results indicate that the proposed framework achieved consistent classification performance across the evaluated metrics. The integration of Faster R-CNN and InceptionV2 enables the extraction of hierarchical image representations and identification of candidate cellular regions, while BLS provides the final classification mechanism through

mapped feature nodes and enhancement nodes.

The confusion matrix presented in Figure 4 provides additional insight into the classification performance across the five cervical cell categories: Dyskeratotic, Koilocytotic, Metaplastic, Parabasal, and Superficial-Intermediate. The results indicate that most test images were assigned to their corresponding categories. However, some misclassifications were observed, particularly in the Metaplastic and Koilocytotic categories. These errors may be associated with similarities in cellular morphology, variations in staining characteristics, and overlapping visual patterns between different cervical cell types. Such observations highlight the challenges involved in distinguishing cytological categories using image-based classification techniques.

A comparative evaluation was also conducted using selected classification approaches, including ResNet-LSTM, InceptionNet, TransLSTM, and Fuzzy CNN. As reported in Table 4, the proposed Hybrid TL-BLS framework achieved the highest accuracy of 94.91% among the listed methods. This result suggests that the combination of transfer-learning-based feature representation and BLS classification is a promising approach for the evaluated five-class classification task. Nevertheless, comparisons with existing architectures should be interpreted in consideration of differences in their implementation, preprocessing procedures, training configurations, and evaluation protocols. A controlled comparison using identical data partitions and experimental conditions would provide stronger evidence of the relative advantages of the proposed framework.

The preprocessing strategy also plays an important role in preparing the cervical cell images for classification. The study employed image resizing, Contrast Limited Adaptive Histogram Equalization (CLAHE), Laplacian sharpening, bilateral filtering, and unsharp masking to enhance image contrast and preserve relevant cellular details. These operations were intended to improve the visual representation of cellular structures before feature extraction. Applying the preprocessing configuration consistently across the training, validation, and testing subsets helps maintain a uniform input representation during model development and evaluation.

Despite the promising results, certain limitations should be acknowledged. First, the evaluation was conducted using only the SIPaKMeD dataset, and therefore the generalizability of the framework to other cervical cytology datasets remains to be established. Second, morphological similarities between cervical cell categories can contribute to classification errors. Third, the present study focuses on image-level classification of five cervical cell categories and does not establish patient-level cervical cancer diagnosis, cancer-risk prediction, or clinical screening effectiveness. Furthermore, the reported performance should be interpreted within the specific experimental conditions and dataset partition used in this study.

Future research will focus on validating the proposed framework using independent and clinically representative cervical cytology datasets. Additional experiments involving different imaging conditions, larger datasets, and cross-dataset evaluation could provide further evidence of its robustness and generalization capability. Investigating alternative feature-extraction backbones, improved region-proposal strategies, and optimized BLS configurations may also help enhance classification performance. Overall, the findings indicate that the proposed Hybrid TL-BLS framework offers a promising computational approach for five-class cervical cell-image classification and may support further research into automated cytological image analysis.

Conclusion

This study presented a hybrid DL framework for automated cervical cell image classification using the SIPaKMeD dataset. The proposed model was evaluated using the SIPaKMeD dataset for five-class cervical cell-image classification. The reported results show the importance of combining transfer-learning-based feature representation with Broad Learning System-based classification for automated classification of cervical cell images. However, the present study is limited to image-level classification on the SIPaKMeD dataset and does not establish patient-level cervical cancer diagnosis or risk prediction. Therefore, the reported performance should not be interpreted as direct clinical diagnostic accuracy. Further validation using independent, clinically representative datasets and appropriate external evaluation protocols is required to assess the generalizability and clinical applicability of the proposed framework.

Ethical Approval

Not applicable.

Acknowledgment

None.

Funding

No external funding was received for this research.

Conflicts of Interest

The authors report there are no competing interests to declare.

References

[1] Stanek-Widera A, Borowczak J, Skiba D, Mickael ME, Łazarczyk M, Maniewski M, et al. Artificial Intelligence in Cervical Cytology: Opportunities and Limitations in Screening, Triage, and Diagnostic Support. Diagnostics. 2026;16(10):1541. [DOI: 10.3390/diagnostics16101541]

[2] Priya S, Panigrahi SK, Bansal V, Arnav A, Raj M, Rai P. Artificial intelligence for cervical cancer screening and diagnosis using Pap smear images: a systematic review. J Obstet Gynecol India. 2026;76(3):192-9. [DOI: 10.1007/s13224-026-02352-4]

[3] Wang X, Wang Q, Ding G, Wang J, Tang Y, Feng Y. Artificial intelligence for colposcopic and cytological image analysis in early cervical cancer detection. iScience. 2026;29(2):114627. [DOI: 10.1016/j.isci.2026.114627]

[4] Valles-Coral MA, et al. Application of artificial intelligence in cervical cytology: a systematic review of deep learning models, datasets, and reported metrics. Front Big Data. 2026;8:1678863. [DOI: 10.3389/fdata.2025.1678863]

[5] Mondal J, Chatterjee R, Kumar Gourisaria M, Sahni M, León-Castro E. Cervical cancer classification using a novel hybrid approach. Front Oncol. 2025;15:1703772. [DOI: 10.3389/fonc.2025.1703772]

[6] Zhang Y, Ning C, Yang W. An automatic cervical cell classification model based on improved DenseNet121. Sci Rep. 2025;15(1):1853. [DOI: 10.1038/s41598-025-87953-1]

[7] Kılıç Eİ, Kılıç Ş. Multi-scale feature integration with enhanced cytomorph for high-accuracy cervical cytology classification. PLoS One. 2026;21(6):e0351063. [DOI: 10.1371/journal.pone.0351063]

[8] Coskun G, Akuner MC, Kaplanoglu E. Robust Cell-Level Classification for Liquid-Based Cervical Cytology Using Deep Transfer Learning: A Multi-Source Study Addressing Scanner-Induced Domain Shifts. Bioengineering. 2026;13(3):289. [DOI: 10.3390/bioengineering13030289]

[9] Fang M, Liao B, Lei X, Wu FX. A systematic review on deep learning based methods for cervical cell image analysis. Neurocomputing. 2024;610:128630. [DOI: 10.1016/j.neucom.2024.128630]

[10] SIPaKMeD: A Segmentation and Image Classification Database for Pap Smear Analysis [Dataset]. University of Ioannina; 2017 [cited 2026 Jan 01]. Available from: https://www.cs.uoi.gr/~marina/sipakmed.html

[11] Ramos-Casallas A, Cardona-Mendoza A, Perdomo-Lara SJ, Rico-Mendoza A, Porras-Ramírez A. Performance evaluation of machine learning models in cervical cancer diagnosis: Systematic review and meta-analysis. Eur J Cancer. 2025;229:115768. [DOI: 10.1016/j.ejca.2025.115768]

[12] Tan SL, Selvachandran G, Ding W, Paramesran R, Kotecha K. Cervical Cancer Classification From Pap Smear Images Using Deep Convolutional Neural Network Models. Interdiscip Sci Comput Life Sci. 2024;16(1):16-38. [DOI: 10.1007/s12539-023-00589-5]

[13] Accuracy-Efficiency Trade-offs in Automated Cervical Cytology Classification: A Comparative Evaluation of ViT, DeiT, PiT, and Swin Transformer on SIPaKMeD. Artif Intell Appl Sci. 2026. [DOI:10.69882/adba.ai.2026021]

[14] Chen CLP, Liu Z. Broad Learning System: An Effective and Efficient Incremental Learning System Without the Need for Deep Architecture. IEEE Trans Neural Netw Learn Syst. 2018;29(1):10-24. [DOI: 10.1109/TNNLS.2017.2716952]

[15] Devi S, Adaickalam V. Modelling a novel approach for cervical cancer prediction using pre-trained network model. Int J Syst Assur Eng Manag. 2025. [DOI: 10.1007/s13198-025-03058-y]

[16] Utomo CP, et al. Optimizing Image Preprocessing for AI-Driven Cervical Cancer Diagnosis. Adv Sustain Sci Eng Technol.

2025;7(1):1-11. [DOI: 10.26877/asset.v7i1.1128]

[17] Hasan MN, Shuvo SB, Ankon MMH, Raju SMTU, Siddique N. TransfusionNet: Framework for cervical cancer detection using deep learning with multi-level fusion. Results Eng. 2025;28:107174. [DOI: 10.1016/j.rineng.2025.107174]

[18] Wang B, Zhao Y, Chen CLP. Hybrid Transfer Learning and Broad Learning System for Wearing Mask Detection in the COVID-19 Era. IEEE Trans Instrum Meas. 2021;70:5004210. [DOI: 10.1109/TIM.2021.3069844]